Electronic and optical properties of δ-layer GaN/(GaAs)$_n$ superlattices

Xuan Luo,* S. B. Zhang, and Su-Huai Wei
National Renewable Energy Laboratory, Golden, Colorado 80401, USA

(Received 12 December 2002; revised manuscript received 26 March 2003; published 9 June 2003)

First-principles total energy calculations reveal qualitative differences between δ-layer GaN/(GaAs)$_n$ superlattices and their corresponding random alloys. Whereas the optical bowing coefficient for the superlattices is typically 30% smaller than that of the alloys with the same concentration, the optical transition matrix elements are comparable to that of GaAs(GaN) and show only weak dependence on nitrogen concentration x. This is because the band-edge states are localized near the GaN region. In contrast, in the random alloys, whereas the conduction band-edge is localized on the N site, the valence band-edge states are increasingly localized into the GaAs-rich region, resulting in significant decrease in optical transitions with increasing x.

DOI: 10.1103/PhysRevB.67.235305 PACS number(s): 73.21.Cd, 71.55.Eq, 71.20.−b, 78.66.Fd

Direct-gap GaAs and GaN are important optoelectronic materials. Because the band gaps of GaAs and GaN are 1.5 and 3.4 eV, respectively, the $GaAs_{1-x}N_x$ alloy is a promising light-emitting material covering the entire visible spectrum. However, it has been observed that with only a small amount of N, the GaAsN random alloys actually show considerable redshift (instead of the blueshift) in the optical transition.[1] This discovery has lead to intense study of the dilute GaAsN alloys in the low-gap (infrared) regime. The physical mechanism of the redshift has been explained in terms of a giant optical bowing caused by the large size and electronegativity differences between nitrogen and arsenic,[2,3] although the physical origin of the conduction band-edge states is still under intense debate.[4–6] A theoretical study[7] also showed that the optical transition matrix elements depend strongly on nitrogen concentration x, being large when $x\sim 0$, but almost zero when $x=20\%$. Clearly, such a strong dependence is a drawback, as it hinders many potential optoelectronic applications. Attempts have been made to improve the optical properties by fabricating short-period $(GaN)_m/(GaAs)_n$ superlattices, as cubic GaN can be grown on the GaAs(001) substrate[8,9] with a critical layer thickness $m\sim 1$ monolayer for pure GaN (Ref. 10) and larger for alloys. For the GaInAsN systems, it has been shown that the short-period superlattices can increase the photoluminescence by a factor up to twelvefold with respect to the random alloys.[11] To date, however, the physical origin of the large enhancement is largely unexplained.

Using first-principles total energy calculations, we study the electronic and optical properties of δ-layer GaN/(GaAs)$_n$ superlattices for $n=3$ to 15 or, equivalently, for $x=6.25$–25%. We find that the superlattices have qualitatively different physical properties than the random alloys. These include the following. (i) The supperlattices exhibit a 30% smaller optical bowing coefficient than that of the alloys. (ii) The band-edge states of the superlattices are localized near the GaN region, a result that depends only weakly on the GaAs layer thickness n. As such, the conduction band-edge state never approaches that of GaAs, no matter how large the n (or how small the x). In contrast, in the random alloys the conduction band minimum (CBM) state becomes delocalized from the GaN region in the N impurity limit, so no gap state remains. (iii) The calculated optical transition matrix elements of the superlattices, being nearly a constant of 0.2 a.u., are comparable to those of GaAs. This is in sharp contrast to the random alloys, where a strong dependence of the matrix elements on x has been predicted.

Our first-principles calculations were carried out within the framework of the density-functional theory. We used the local density approximation (LDA) (Ref. 12) for the exchange-correlation energy functional and a plane-wave expansion for the basis set. Extensive structural relaxations were carried out with the VASP code[13] and the ultrasoft vanderbilt pseudopotentials[14] with a cutoff energy of 450 eV. For the optical properties, we used the LBNL code[15] and the Troulier-Martins potential with a 40 Ry cutoff energy. For the Brillouin zone integration, we used the equivalent k-point scheme (i.e., we used the k points that are equivalent to the ten special k point for the zinc blende cell). Upon relaxation of the c/a ratio, however, the k-point mesh was kept unchanged. The in-plane lattice constant used in the calculations is that of the GaAs substrate 5.587 Å. All the atoms were fully relaxed, with the remaining atomic forces less than 0.05 eV/Å. The total energy is converged to less than 5 meV per 32-atom supercell. We obtained $c/a\approx(n-1)/2+0.78$ for any odd number n between 3 and 15. It is well known that the LDA underestimates the band gap. In the following, we have corrected the band gaps of GaAs and GaN according to the experimental values 1.52 and 3.4 eV, respectively. For the superlattices, we used a linear interpolation scheme with respect to x to obtain the band gap corrections.

Figure 2(a) shows by filled circles, the calculated energies of the valence band maximum (VBM) and CBM states as a function of N concentration x with respect to those of GaAs. For VBM, we assume they follow the same trend as predicted by the effective mass model (see below). Separately, Fig. 2(b) shows the band gap change as a function of x. We see that much of the band gap change takes place in the conduction band rather than the valence band. To gain further understanding of these energy changes, we carried out an effective-mass model calculation in which we consider an electron/hole in a one-dimensional periodic potential.[16] To construct the potential, we calculated the band offset between GaAs and epitaxially *strained* GaN by using the general potential, all electron, linearized augmented plane wave

 ©2003 The American Physical Society

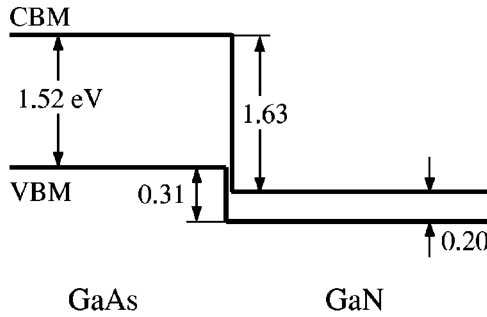

FIG. 1. The calculated type-III band offset between GaAs and epitaxially GaN by using LAPW method. The conduction band offset $\Delta E_c = 1.63$ eV and the valence band offset $\Delta E_v = 0.31$ eV.

(LAPW) method,[17] shown in Fig. 1. We obtain a type-III band alignment with the conduction band offset $\Delta E_c = 1.63$ eV and the valence band offset $\Delta E_v = 0.31$ eV. We also use $m^e_{\mathrm{GaN}} = 0.2m_0$ and $m^e_{\mathrm{GaAs}} = 0.067m_0$ for the conduction electron states, where m_0 is the free electron mass, and $m^h_{\mathrm{GaN}} = 0.6m_0$ and $m^h_{\mathrm{GaAs}} = 0.53m_0$ are the valence hole states. All the m^*'s are taken from experiment[18] or first-principles calculations.[19] The results of the effective-mass calculations are shown in Fig. 2(a) by the open triangles. Because the valence band offset is small and the hole wave function is more localized on GaAs, the results are not very sensitive to the hole effective mass used here. The agreement between the effective-mass model and the first-principles calculations is reasonable. This suggests that (a) the gap correction scheme used in the direct calculation is reasonable, as the effective-mass model does not involve any such corrections. (b) Quantum confinement is solely responsible for the gap change in the superlattices. Also, an interesting prediction of the effective-mass calculations is that, due to the relatively large conduction band offset, the energy level of the lowest conduction band state in the superlattice will *never* reach the bulk GaAs conduction band edge, no matter how large the n or how small the x. This is in contrast to GaAsN random alloys, where the conduction band edge is expected to approach that of GaAs in the N impurity limit.

Figure 2(b) shows the calculated band gaps for the superlattices (filled circles) versus the band gaps of the random alloys calculated previously[7] by an empirical pseudopotential method (EPM) (open circles).[20] Both the superlattices and the random alloys show significant band gap reductions, as demonstrated in Fig. 2(c) by the large bowing coefficients $b(x) = \triangle E_g(x)/x(x-1)$, where $\triangle E_g(x)$ is the deviation of the calculated gap from the linear average of the constitute band gap.

However, there are also important differences. Noticeably, the bowing coefficients for the random alloys are about 30% larger than those of the superlattices. As a result, for example, to obtain a 1.1-eV band gap for either photovoltaic or long-wavelength laser applications, one needs $x \sim 17\%$ or a $(\mathrm{GaAs})_5/\mathrm{GaN}$ superlattice, but for random alloy, $x \sim 10\%$ is sufficient. Figure 3 shows the wave function squared (or charge) for the conduction and valence band-edge states for $n = 3$, 7, and 15 ($x = 25$, 12.5, and 6.25 %), respectively. We see from Fig. 3 that both the VBM and CBM states have significant fractions localized near the GaN region, irrespective of the thickness of the GaAs layer n. The total amount of charge *within* one GaN layer increases with n (or in other words decreases with x), even though the percentage in the entire GaN region decreases with n. In contrast, previous study for the random alloys showed that only the CBM state remains to be localized near the nitrogen region whereas the VBM state is increasingly more localized in the As region when x increases.[7] The reason that the VBM of the superlattice is localized on the N layer is mainly caused by the large c/a distortion in the GaN layer, which lead to the Γ_4 state move much higher above the Γ_5 state. It has been suggested that a strong localization of the CBM state in the GaN region is the reason for the large bowing in the random GaAsN alloys.[2] In the present case, however, although the CBM state of the superlattices shows clear localization near the GaN region, a significant amount of the charge can also be seen in the GaAs region. Hence, the smaller bowing coefficients for the superlattices could be attributed to less localization of the CBM states in the GaN region.

Recently, the EPM approach has also been applied to the

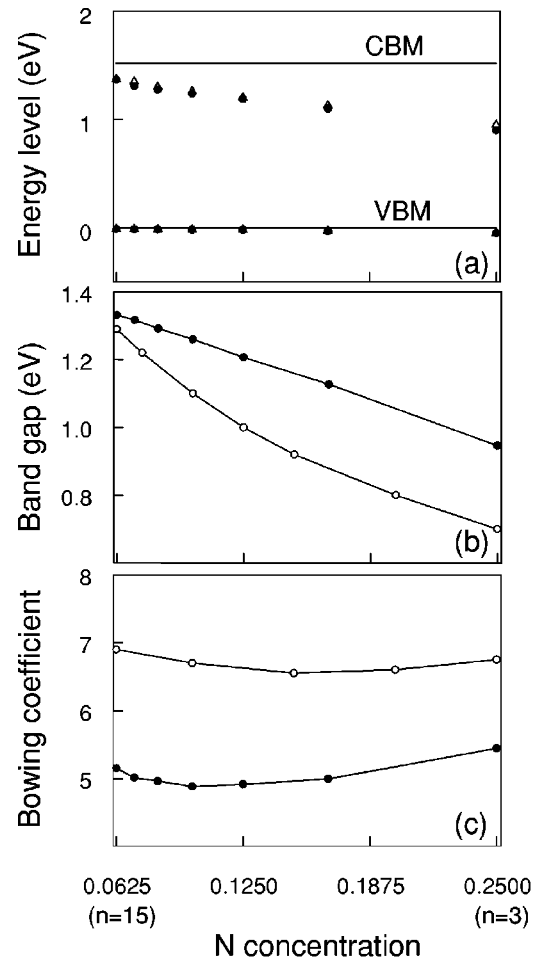

FIG. 2. Calculated (a) energy of band-edge states with respect to the GaAs VBM and CBM (solid lines), (b) the band gap, and (c) the bowing coefficient for δ-layer GaN/$(\mathrm{GaAs})_n$ superlattices (filled circles). For comparison, the results of an effective mass model [open triangles in (a)] and those of an EPM calculation for the random alloys [open circles in (b) and (c)] are also shown.

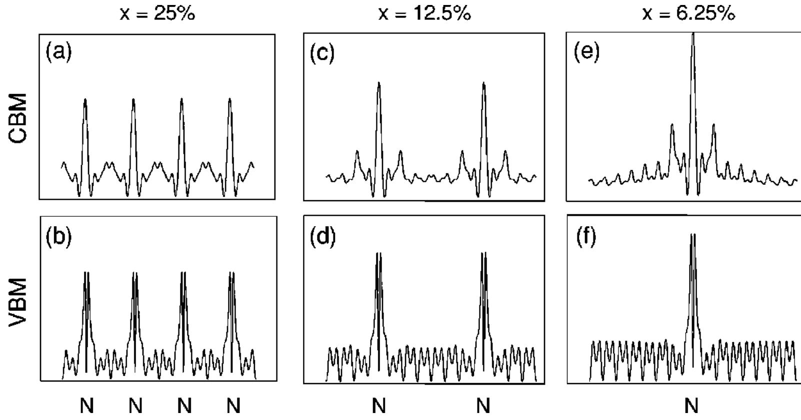

FIG. 3. Planar averaged charge densities for CBM and VBM states, respectively, for δ-layer GaN/$(GaAs)_n$ superlattices. (a) and (b) are for $n=3$ ($x=25\%$); (c) and (d) are for $n=7$ ($x=12.5\%$); and (e) and (f) are for $n=15$ ($x=6.25\%$).

δ-layer GaN/$(GaAs)_n$ superlattices.[21] Smaller band gaps, and hence larger bowing coefficients, have been predicted than those being reported here: for example, 0.775 eV for the $(GaAs)_{14}/GaN_{strained}$ superlattice, while we obtain 1.32 eV for the $(GaAs)_{15}/GaN$ and 1.23 eV for the $(GaAs)_{13}/GaN$ superlattices, respectively. The problem with the EPM calculations lies in the use of incorrect band offsets between GaAs and GaN. The GaN is strained on the GaAs substrate, thus, strained values, such as the one obtained here from first-principles calculation, should be used. Using the band offsets for the strained systems, however, our effective mass model does not support the previous EPM results, but is in good agreement with our first-principles results that, of course, do not need any band offset as input.

Figure 4(a) shows, by filled circles, the calculated optical-transition matrix elements squared between the band-edge states at Γ. They are defined as

$$M=|\langle \psi_v(\mathbf{k,r})|\mathbf{P}|\psi_c(\mathbf{k,r})\rangle|^2=\left|\sum_G \mathbf{G}C_v(\mathbf{G})C_c^*(\mathbf{G})\right|^2, \quad (1)$$

where $\mathbf{P}$ is the momentum operator and $|\psi_s(\mathbf{k,r})\rangle=\Sigma_G C_s(\mathbf{k,G})e^{i(\mathbf{k+G})\cdot\mathbf{r}}$, with $s=v$ or c as the VBM and CBM wave functions, respectively. For comparison, we also calculated M for bulk GaAs, as well as for unstrained and strained bulk GaN. They are 0.286, 0.433, and 0.299 a.u., respectively. Hence, we find that formation of the superlattices has only a modest effect on optical properties, which are not sensitive to the GaAs layer thickness. This is, in fact, highly desirable for optical applications. In contrast, Fig. 4(a) also shows, by open circles, the matrix element M for the $GaAs_{1-x}N_x$ random alloys, calculated by the EPM method. Here, M is instead a strong function of x, being reduced initially at a rate of about 0.014 a.u. for every 1% increase in x and to become nearly zero for $x=25\%$. To understand the variation of the M with x for the superlattices, we study in Fig. 4(b) the product of the VBM and CBM states, defined as $P=\int\langle\psi_v(z)|\psi_v(z)\rangle\langle\psi_c(z)|\psi_c(z)\rangle dz$. The quantity P here reflects the degree of spatial charge overlap between the VBM and CBM states. If P is small, the wave function overlap $\int\langle\psi_v(z)|\psi_c(z)\rangle dz$ would also be small. So, too, is M [see Eq. (1)]. Figure 4(b) shows, by open triangles, filled circles, and filled squares, the calculated Ps in the GaN and GaAs (sub)regions and for the superlattices as a whole. Reflecting the strong localization of both the CBM and VBM states in the GaN region in Fig. 3, the product P in Fig. 4(b) is significant and increases noticeably with x in the GaN region and, hence, in the entire superlattices. The situation for the random alloys is, however, qualitatively different, as the VBM state is more and more localized in the GaAs region with increasing x, while the CBM state remains very much in the GaN region except in the N impurity limit.

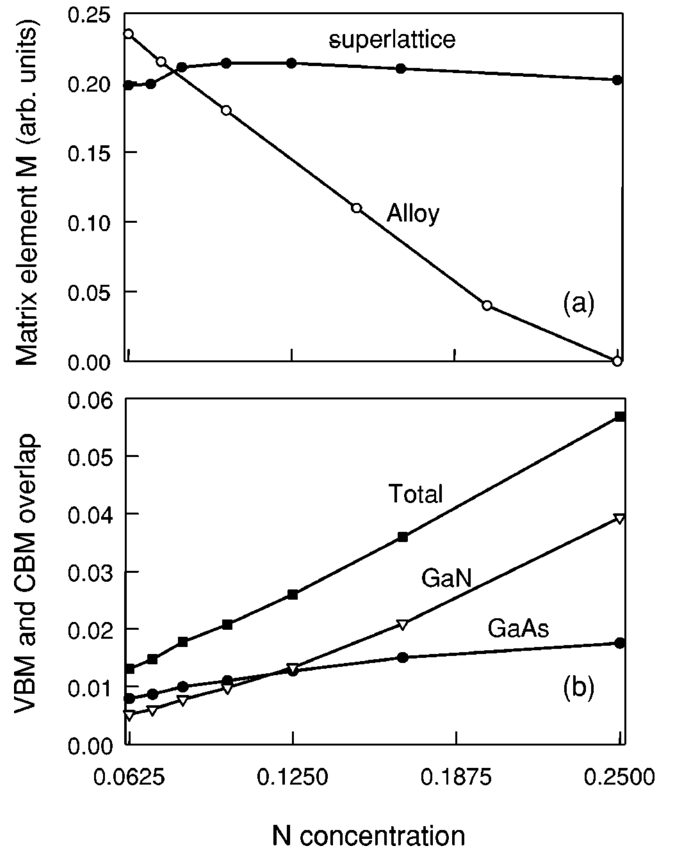

FIG. 4. (a) Calculated dipole transition matrix elements as a function of x. The filled circles are for the δ-layer GaN/$(GaAs)_n$ superlattices, whereas the open circles are for the $GaAs_{1-x}N_x$ random alloys, calculated by an empirical pseudopotential method. (b) The products of the wave function squared of the VBM and CBM as a function of x, for the GaN region (open triangles), the GaAs region (filled circles), and the entire superlattices (filled squares).

Hence, M decreases with x. From the above analysis, one might expect that M for the superlattices should also increase with x, but the actual result in Fig. 4(a) instead shows a saturation. We find that this is a result of intermixing between the Γ-derived CBM (Γ_{1c}) state and the X-derived (X_{3c}) states folded to the $\bar{\Gamma}$. The intermixing, which is larger for smaller period n, takes away spectra weight from the Γ transition and puts it into the forbidden Γ-X_{3c} transition. As a result, the overall optical transition matrix element decreases slightly with decreasing n or increasing x.

In summary, we studied the electronic and optical properties of δ-layer GaN/$(GaAs)_n$ superlattices using first-principles methods and compared them with random GaAsN alloys. Qualitative differences in the electronic and optical properties are identified. Whereas smaller bowing coefficients are generally expected for the superlattices, their optical-transition matrix elements show only weak dependence on the nitrogen concentration x. This makes the δ-layer GaN/$(GaAs)_n$ superlattices potentially useful for optical applications, because for the random alloys, M decreases drastically as x increases.

This work was supported by the U.S. DOE-SC-BES under Contract No. DE-AC36-99GO10337 and by the MPP Supercomputer time at NERSC.

*Email: xluo3@uiuc.edu

[1] M. Weyers, M. Sato, and H. Ando, Jpn. J. Appl. Phys. **31**, L853 (1992).

[2] S.-H. Wei and A. Zunger, Phys. Rev. Lett. **76**, 664 (1996).

[3] J. Neugebauer and C. G. Van de Walle, Phys. Rev. B **51**, 10 568 (1995).

[4] T. Mattila, S.-H. Wei, and A. Zunger, Phys. Rev. B **60**, R11 245 (1999).

[5] W. Shan *et al.*, Phys. Rev. Lett. **82**, 1221 (1999).

[6] Y. Zhang, A. Mascarenhas, H. P. Xin, and C. W. Tu, Phys. Rev. B **61**, 7479 (2000).

[7] L. Bellaiche, S.-H. Wei, and Alex Zunger, Phys. Rev. B **54**, 17 568 (1996); **56**, 10 233 (1997).

[8] L. W. Sung, H. H. Lin, and C. T. Chia, J. Cryst. Growth **241**, 320 (2002).

[9] A. Bensaoula, W. T. Taferner, E. Kim, and A. Bousetta, J. Cryst. Growth **164**, 185 (1996).

[10] M. Sato, Surf. Sci. Spectra **41**, 323 (1997).

[11] Y. G. Hong, A. Egorov, and C. W. Tu, J. Vac. Sci. Technol. B **20**, 1163 (2002).

[12] W. Kohn and L. J. Sham, Phys. Rev. **140**, A1133 (1965).

[13] G. Kresse and J. Hafner, Phys. Rev. B **47**, 558 (1993).

[14] D. Vanderbilt, Phys. Rev. B **41**, 7892 (1990).

[15] The PETOT code, developed by L. W. Wang of LBNL can be downloaded from http://www.nersc.gov/ linwang

[16] S. B. Zhang, M. L. Cohen, and S. G. Louie, Phys. Rev. B **43**, 9951 (1991).

[17] S.-H. Wei and H. Krakauer, Phys. Rev. Lett. **55**, 1200 (1985).

[18] *Semiconductors Basic Data*, edited by O. Madelung (Springer-Verlag, Berlin, 1996).

[19] G. D. Chen *et al.*, Appl. Phys. Lett. **68**, 2784 (1996).

[20] Previous calculations show similar results between EPM and LDA for the random alloys, reflecting the use of the LDA results as input in the EPM parametrization. See, for example, T. Mattila, Su-Huai Wei, and A. Zunger, Phys. Rev. B **60**, R11 245 (1999); L. Bellaiche and A. Zunger, *ibid.* **57**, 4425 (1998); P. R. C. Kent and A. Zunger, *ibid.* **64**, 115208 (2001).

[21] H. Schmidt and R. Pickenhain, Phys. Rev. B **65**, 045323 (2002).